

Figure S1 The Human Extraembryonic Compartment, Related to Figures 3 and 5. **A**, A human placenta with portions of the fetal membranes. Chorionic villi are the functional units of the placenta. The histology of the boxed areas is shown in the panels with the corresponding letters. **B**, View of the fetal membranes at the cellular level. The amnion is composed of a single epithelial layer, which lines the amniotic cavity, and an underlying stroma. The smooth chorion, which shares the stromal compartment, contains multiple layers of cytotrophoblasts. The outer rank of cells lies adjacent to the uterus. The scissors depict where the membranes were bisected, producing the amnion and smooth chorion samples. **C**, View of the maternal-fetal interface at the cellular level. The mononuclear cytotrophoblast layer of the (early gestation) chorionic villi fuses to become multinuclear syncytiotrophoblasts, which form the surface of the placenta. Floating villi are perfused by maternal blood that fills the intervillous space. Anchoring villi give rise to invasive extravillous cytotrophoblasts that emigrate from the chorionic villi via cell columns that attach the placenta to the uterus and infiltrate most of its wall. Maternal cells in this region include the decidua, remodeled uterine blood vessels, which are lined by cytotrophoblasts, and immune cells. During vascular invasion, the cells breach both veins and arteries, but they have much more extensive interactions with the arterial portion of the uterine vasculature. Here, they replace the endothelial lining and intercalate within the smooth muscle walls of the spiral arteries, producing hybrid vessels that are composed of both embryonic/fetal and maternal cells. Vascular invasion connects the uterine circulation to the intervillous space where maternal blood perfuses the chorionic villi.

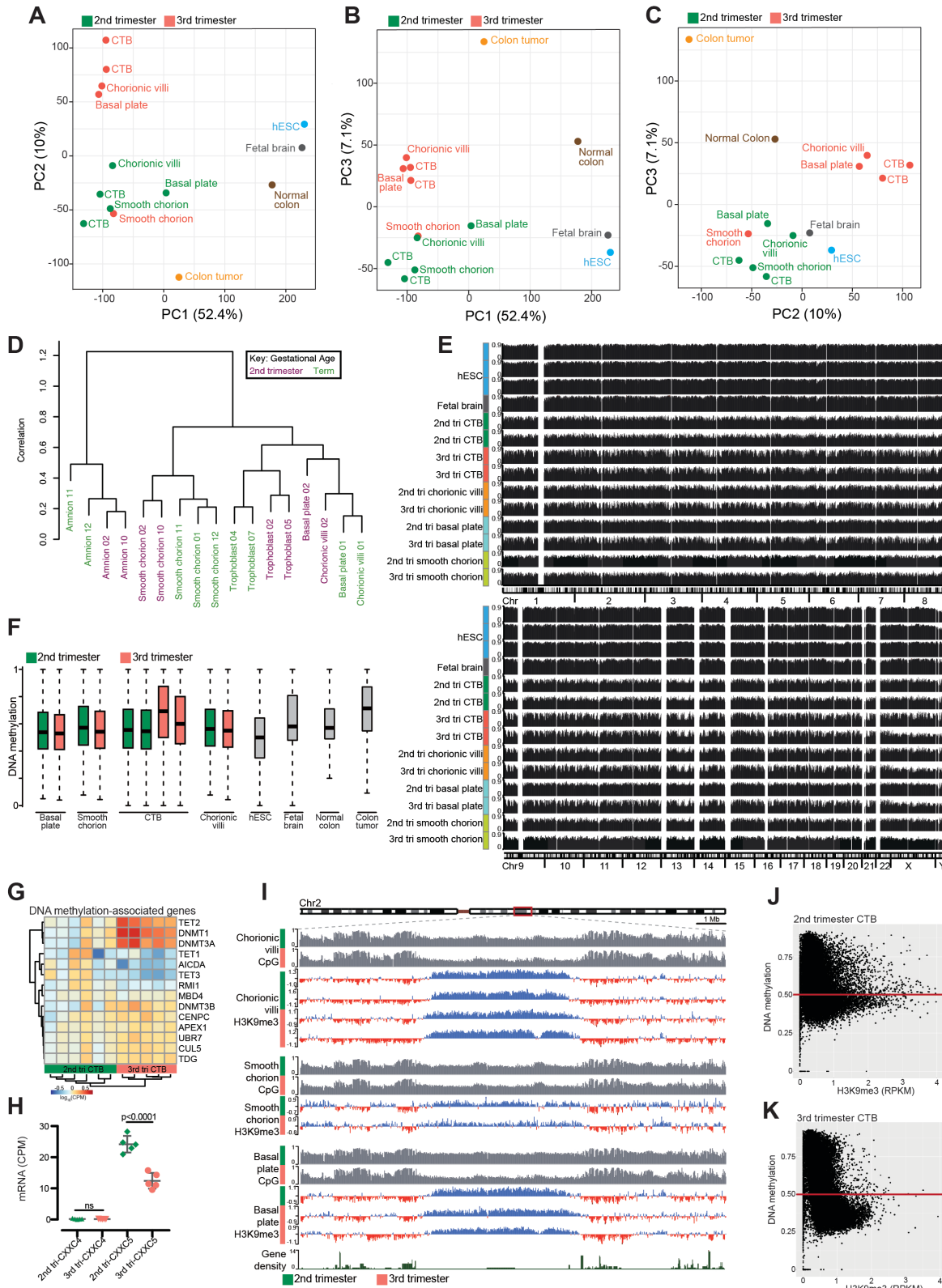


Figure S2 DNA Methylation patterns of Extraembryonic Tissues and Cytotrophoblasts, Related to Figure 1. A-C, The principal component analyses depicting the whole genome bisulfite-seq data. D, DNA methylation array data confirmed the whole-genome bisulfite-seq data. Samples clustered according to their type and gestational age. The only exceptions were basal plate and chorionic villi, which contained many of the same cell types. E, Chromosome-level view of DNA methylation across the genome of the extraembryonic compartments. The height of the colored bars corresponds to the number of different samples of each type that are shown. The white empty strips are heterochromatin/centromeric regions with poorly aligned, repetitive sequences, thus they were left blank. F, DNA methylation in imprinting control regions. Imprinting control regions of the extraembryonic genomes had methylation levels centered near 50% as the other samples. The colored bodies of the box plots represent the first and third quartiles of loci, the middle line represents the

median, and the whiskers extend to the minimum and maximum data points. **G**, Cytotrophoblast mRNA levels of DNA methylating and demethylating enzymes. Note the expression of *DNMT1* and *DNMT3A*, DNA methyltransferases, was higher at term. Whereas, *TET1* and *TET3*, DNA demethylating proteins, were expressed less at term. **H**, TET2 was expressed more at term; however, the potential CXXC-containing TET2 co-factors were either not expressed (*CXXC4*) or downregulated (*CXXC5*) in 3rd trimester cytotrophoblasts. **I**, A chromosome-level (Chr2) view showed that deeply hypomethylated domains of the 2nd and 3rd trimester samples from extraembryonic compartment were occupied by H3K9me3. **J-K**, Scatter plots of DNA methylation levels vs. H3K9me3 occupancy in 2nd and 3rd trimester cytotrophoblasts. CTB, cytotrophoblast; hESC, human embryonic stem cells; CTB, cytotrophoblast; tri, trimester; Chr, chromosome.

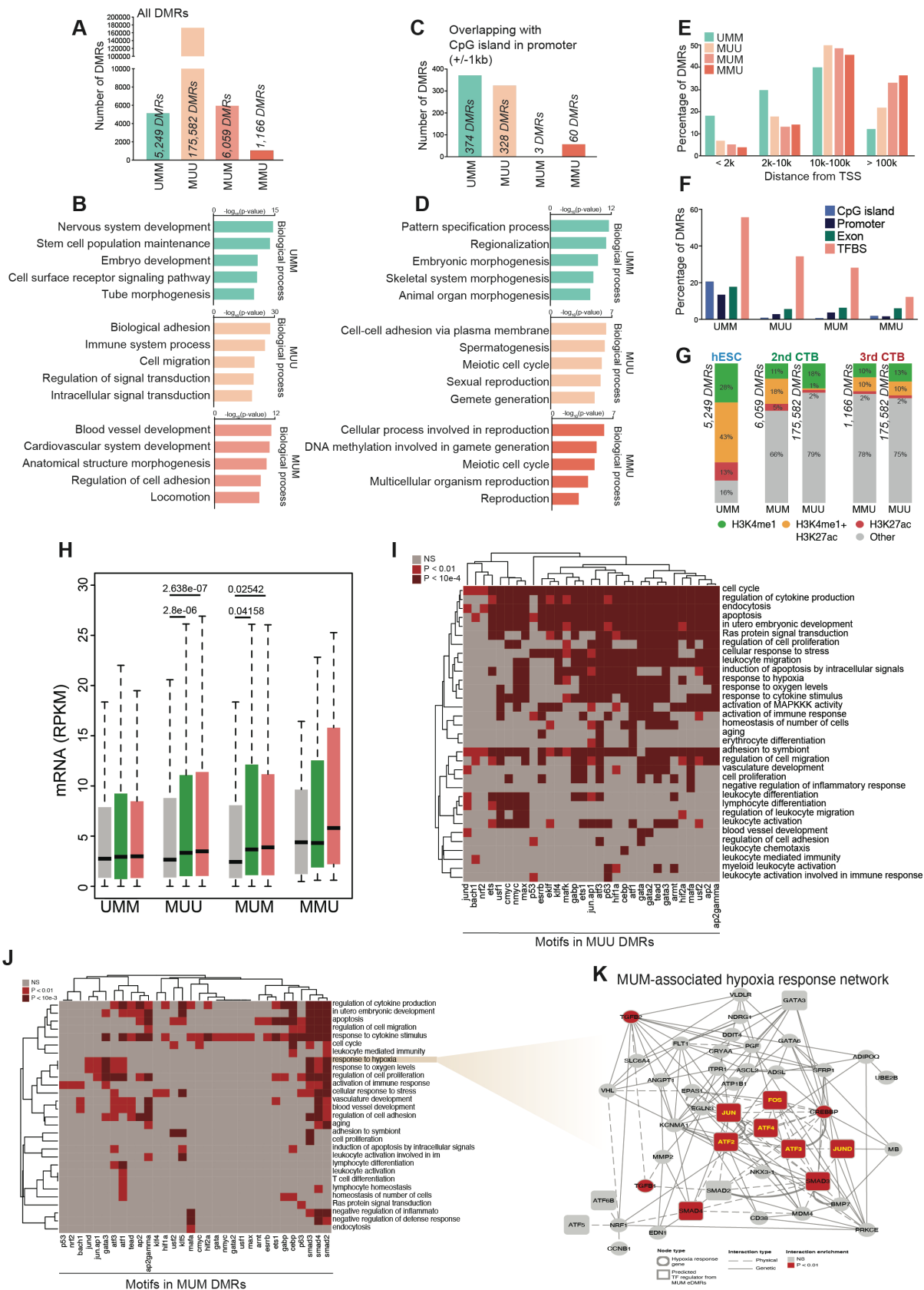


Figure S3 Characteristics of the Unmethylated Regions of the Cytotrophoblast Genome as Compared to Human Embryonic Stem Cells, Related to Figure 2. **A**, Differentially methylated regions (DMRs) were categorized according to whether they were methylated (M) or unmethylated (U) in human embryonic stem cells (hESCs) relative to 2nd or 3rd trimester cytotrophoblasts (CTBs). **B**, GO analyses of the sites that were uniquely hypomethylated in hESCs (UMM) revealed biological processes that are associated with embryonic morphogenesis. In contrast, GO analyses of the sites that were uniquely hypomethylated in CTBs (MUU) yielded terms related to cell adhesion or migration, immune processes

and signal transduction. GO analyses of sites that were uniquely hypomethylated in 2nd trimester CTBs (MUM), revealed cardiovascular development and cell adhesion or locomotion. **C**, In contrast to global methylation, hESCs and CTBs had relatively equivalent numbers of hypomethylated DMRs in the CpG islands of gene promoters. **D**, GO analyses of these sites highlighted embryonic and reproductive processes, respectively. **E-F**, As compared to hESCs, a larger percentage of CTB DMRs (MUU, MUM, MMU) were distant from **E** the transcription start sites (TSS) and **F** contained transcription factor binding sites (TFBS). **G**, Enhancer DMRs with H3K27ac and/or H3K4me1. **H**, Expression levels of genes that interact with enhancer DMRs predicted by EnhancerAtlas. Unless marked, the values were not significantly different from one another (ANOVA). **I**, In the MUU dataset, genes near enhancer-DMRs (eDMRs; DMR, differentially methylated region) containing transcription factor binding motifs were enriched for functions related to the cell cycle, regulation of cytokine production, endocytosis, apoptosis, *in utero* embryonic development, RAS signaling, cellular stress, migration, hypoxia/oxygen responses, and adhesion, among others. **J**, The heatmap of predicted transcription factor binding motifs and putative target gene pathways in the MUM dataset, which included many of the same pathways shown in **A**, but fewer transcription factor motifs, suggesting down-regulation at term. **K**, Network of AP-1 and SMAD in hypoxia response. Independent experimental data was used to assemble a network of validated genetic and physical interactions between the candidate transcription factor regulators and hypoxia response target genes (Chatr-Aryamontri et al., 2013; Rankin and Giaccia, 2016). Hypoxia inducible factor motifs were not associated with hypoxia response in MUM eDMRs, perhaps due to the fact that HIF regulation occurs at the protein level (Rankin and Giaccia, 2016). Predicted transcription factor regulators—particularly SMAD3, SMAD4, and the AP-1 complex—had more interactions in the hypoxia response network than expected by chance. Six of the 11 most significantly connected genes in the network were Transcription factors predicted by motifs in MUM eDMRs ($P < 0.01$, hypergeometric; yellow lettering). Thus, in addition to the hypoxia response regulators associated with MUU eDMRs, AP-1, SMAD3, and SMAD4 binding at MUM eDMRs may be of particular importance for cytotrophoblast (CTB) hypoxia responses. Potential interactors in this network included VHL, which, under normoxic conditions, targets HIFs for ubiquitinylation and proteasomal degradation. VHL mutations are associated with renal cell carcinomas (Gossage et al., 2015). CTBs express this molecule, which is regulated by O₂ levels and as a function of differentiation (Genbacev et al., 2001).

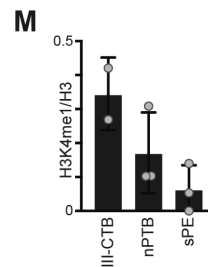
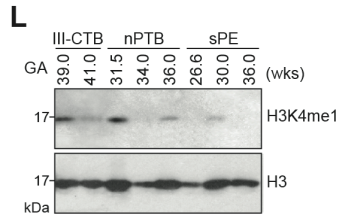
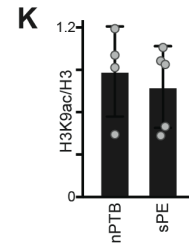
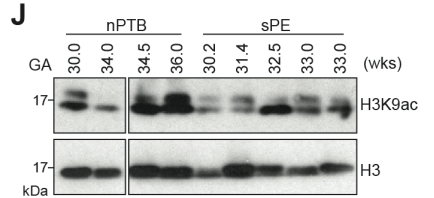
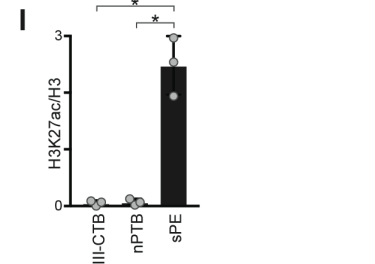
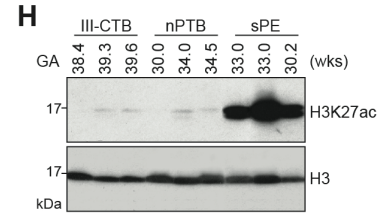
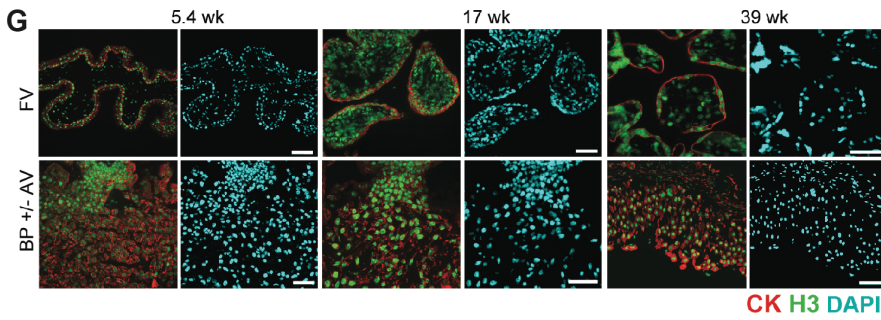
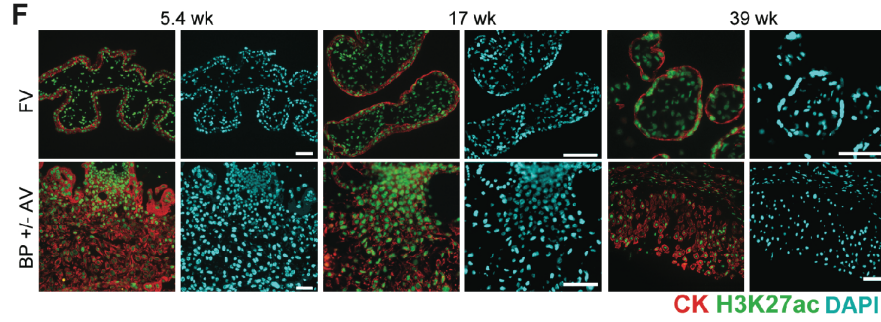
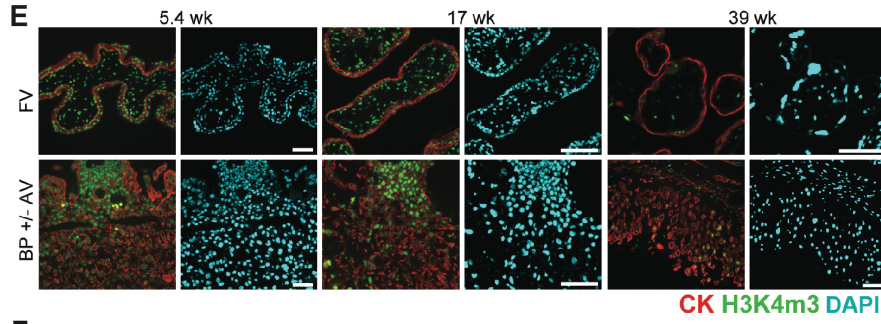
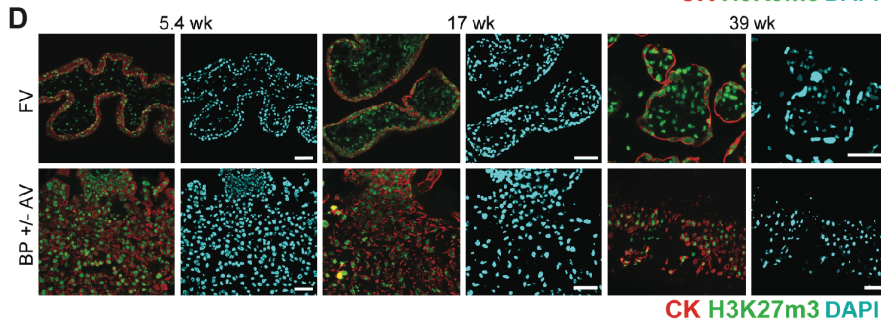
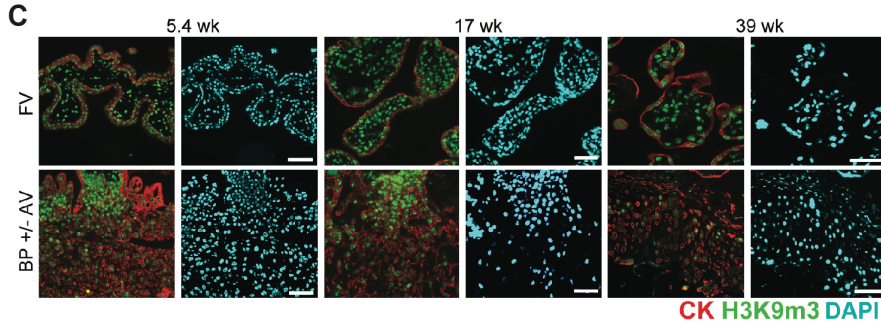
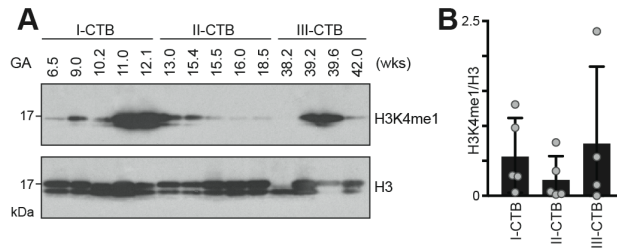


Figure S4 Immunoblots and Immunolocalizations of Modified Histones in Cytotrophoblasts, Related to Figures 3 and 5. **A-B,** A) CTB H3K4me1 expression across gestation and B) quantification of the immunoblot signals. **C-G,** Samples with nearly identical morphology were 5 μ m serial sections. In other cases, the immediately adjacent sections were lost, which resulted in greater morphological differences among the tissue sections. **C)** (upper panels) In floating villi (FV), the nuclei of cytokeratin-positive villous cytotrophoblasts (CTBs) and syncytiotrophoblasts (STBs) reacted with anti-H3K9me3 in the 1st and the 2nd trimester samples. Much of the immunoreactivity was lost at term. (lower panels) In anchoring villi (AV) and within the basal plate (BP), invasive CTBs showed a similar pattern of down-regulated H3K9me3 at term. **D-E)** In FV and BP \pm AV, CTB (and STB) signals for H3K27me3 and H3K4me3 were also diminished at term. **F)** Compared to the immunoblot (Figure 3E), relatively strong H3K27ac signals were observed in association with trophoblasts in floating and anchoring villi and the staining was again reduced at term. **G)** Immunolocalization of total histone H3 confirmed the patterns shown in panels (C-F) as indicative of the relative abundance of the histone modifications that were analyzed rather than altered levels of the protein. **H-I,** Cytotrophoblasts from normal births at term (III-CTB), similar to those from pregnancies that ended in a (non-infected) preterm birth, had low-to-no bands that reacted with anti-H3K27ac as compared to the CTB lysates from placentas of patients with severe preeclampsia (sPE). **J-M,** Immunoblotting with H3K9ac or H3K4me1 revealed bands of variable intensities that were not specific to nPTB or sPE. The error bars represent the standard deviations. Unless marked with asterisks (Welch's t-test; *, $P < 0.05$), the values were not significantly different from one another. GA, gestational age; wks, weeks; I, first trimester; II, second trimester; III, third trimester.

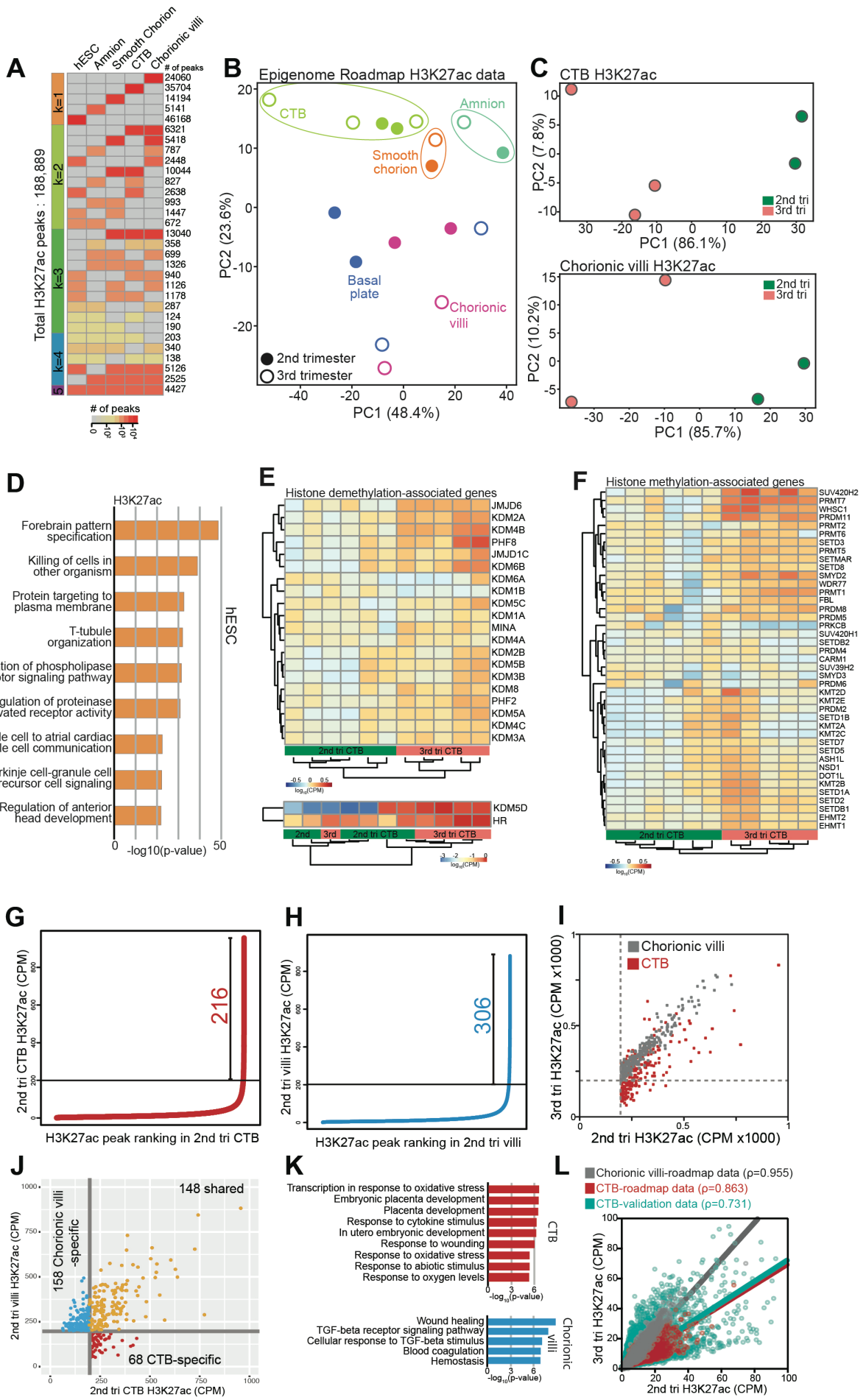


Figure S5 Characterization of H3K27ac in Cytotrophoblasts and Other Regions of the Extraembryonic Compartment, Related to Figure 4. **A**, Number of H3K27ac peaks that were unique to each cell type/region or co-occurred in more than one dataset. **B**, Principal component analysis of 10 kb windows separated the samples according to type except for the basal plate and villi, which contained many of the same cell types. **C**, As to individual sample types, PCA of 10 kb windows separated CTBs and chorionic villi by gestational age. **D**, GO terms associated with human embryonic stem cell (hESC)-specific H3K27ac peaks. **E-F**, Gene lists were obtained from epifactor: <http://epifactors.autosome.ru/>; n=6, 2nd trimester; n=5, 3rd trimester. **E**) Enzymes associated with histone demethylation. *KDM5D* and *HR* data were shown separately due to their higher expression levels. **F**) Enzymes associated with histone methylation. **G-H**, Ranking the H3K27ac signal density, 216 and 306 super-enhancers were identified in 2nd trimester cytotrophoblasts (CTBs) and villi, respectively. **I**, A large set of 2nd trimester CTB super-enhancers lost H3K27ac at term; gestational age-related shifts were not observed in villi. **J**, Many super-enhancers were shared between the two sample types (148; gold); others were unique to villi (158; blue) or CTBs (68; red). **K**, Genes near CTB-specific super-enhancers were highly enriched in functions related to oxidative stress and placental development. Genes near villi-specific enhancers were unique in terms of TGF-beta-related functions, and roles in wound healing, coagulation and hemostasis. **L**, Scatter plots of 10 kb windows confirmed the preferential loss of H3K27ac in CTBs vs. villi in the additional samples (new H3K27ac datasets). Linear regression lines and Pearson's ρ shows the correlation between 2nd and 3rd trimester H3K27ac levels. tri, trimester.

Figure S6 Transcriptomes of cytotrophoblasts and various extraembryonic compartments during the 2nd and 3rd trimesters, Related to Figure 4. **A**, Principal component analysis depicting the mRNA transcriptomes of the five sample types analyzed at two gestational ages. **B**, Correlation heatmap of the transcriptomes shown in A. **C**, GO enrichment and KEGG pathway analyses revealed potential functional enrichments by cell type/compartiment. **D**, Cytotrophoblasts (CTBs) had significantly different miRNA expression patterns as compared to the other samples. **E**, Differentially expressed cytotrophoblast genes between 2nd and 3rd trimester CTBs. tri, trimester.

Table S1 Number of DMRs, eDMRs, and genes associated with eDMRs. Related to Figures 2 and S3.

A. DMRs and eDMRs identified

Methylated (M) or unmethylated (U) in hESCs vs 2nd trimester CTBs vs 3rd trimester CTBs	Total DMRs	DMRs with H3K27ac and/or H3K4me1 (eDMRs)	eDMRs in 10 kb of genes	Genes associated with eDMRs	Genes associated with multiple eDMRs	Expressed genes associated with eDMRs
UMM	5249	4416	1590	1143	283	389
MUU	175582	38887	12139	6891	2751	2521
MUM	6059	2040	651	581	64	208
MMU	1166	294	82	79	3	31

B. eDMRs and their associated genes identified using EnhancerAtlas

Methylated (M) or unmethylated (U) in hESCs vs 2nd trimester CTBs vs 3rd trimester CTBs	Total DMRs	DMRs with H3K27ac and/or H3K4me1 (eDMRs)	eDMRs filtered with EnhancerAtlas and within 50kb of TSSs	# of expressed genes associated with eDMRs	Average # eDMRs associated with a gene
UMM	5249	4416	1067	478	2.2
MUU	175582	38887	9212	2929	3.1
MUM	6059	2040	484	280	1.7
MMU	1166	294	60	36	1.7

Table S2 Maternal/neonatal clinical characteristics and antibodies employed. Related to Figures 3, 5 and 6.

Table S2A. Maternal and neonatal clinical characteristics (immunoblotting and immunolocalization), related to Figure 5

Summary of clinical information			
	PTB (n=6) **	sPE (n=6)	P-value
Ethnicity	6O	4H, 2O	n/a
Maternal age, yr	30.67±7.34	28.83±6.43	0.6552
BMI, kg/m ²	25.8±3.81	35.17±5.25	0.0159
Systolic blood pressure, mmHg	115.6±12.09	163.5±9.77	<0.0001
Diastolic blood pressure, mmHg	68.2±7.79	95.67±8.2	0.0003
Proteinuria (mg/dL)	n/a or 0	81.67±61.88	<0.0001
Gestational age at delivery (days)	232.33±17.92	225.83±7.81	0.4212
Birth weight, g	2220.2±582.27	1740.67±174.72	0.0851
Birth (C/S: SVD)	1C/S : 4SVD	2C/S : 4SVD	0.6618

O = other and H = Hispanic/Latino;
 Mean ± SD; C/S: cesarean section, SVD: spontaneous vaginal delivery
 ** including one infected PTB

Case-by-case clinical information

Diagnosis	Race/Ethnicity	Maternal Age	BMI	Systolic BP	Diastolic BP	Proteinuria	Gestational Age	Birth weight	Delivery method	Fetal sex	Growth %ile	Notes
PTB	na	30	na	na	na	na	30	na	na	na	na	
PTB	Not Hispanic or Latino	23	na	117	67	na	30	1181	C/S	female	3%	growth restricted
PTB	Not Hispanic or Latino	36	29.5	110	60	na	34	2440	NSVD	male	58%	
PTB	Not Hispanic or Latino	39	21.2	101	68	na	34.5	2445	NSVD	female	39%	
PTB	Not Hispanic or Latino	21	24.2	116	65	na	34.3	2500	NSVD	male	54%	
infected PTB	Not Hispanic or Latino	35	28.3	134	81	na	36	2535	NSVD	female	22%	
sPE	Hispanic or Latino	30	29	156	82	54	30.2	1400	C/S	female	15%	
sPE	Not Hispanic or Latino	40	39.5	177	104	62	33	1850	NSVD	male	13%	
sPE	Not Hispanic or Latino	25	40.2	171	101	173	32.5	1765	C/S	female	11%	
sPE	Hispanic or Latino	21	33.7	150	90	21	31.4	1850	NSVD	female	48%	
sPE	Hispanic or Latino	30	39.4	164	100	36	33	1850	NSVD	male	13%	
sPE	Hispanic or Latino	27	29.2	163	97	144	33	1729	NSVD	female	6%	growth restricted

na = not available
 PTB = Preterm birth
 sPE = Severe preeclampsia

Table S2B. Maternal and neonatal clinical characteristics (cytotrophoblast ChIP-seq), related to Figure 6

Summary of clinical information	
	PE (n=6)
Ethnicity	1AA, 3H, 2O
Maternal age, yr	33.33 ± 6.89*
BMI, kg/m ²	35.96 ± 4.27
Systolic blood pressure, mmHg	167.33 ± 19.7
Diastolic blood pressure, mmHg	94.5 ± 10.33
Proteinuria (mg/dL)	84.17 ± 117.07
Gestational age at delivery	31.23 ± 1.91
Birth weight, g	1544.16 ± 410.93
Birth (C/S: SVD)	3 C/S: 3 SVD

O = other, AA = African-American, and H = Hispanic/Latino;
 Mean ± SD; C/S: cesarean section, SVD: spontaneous vaginal delivery

Case-by-case clinical information

Sample ID	Race/Ethnicity	Maternal Age	BMI	Systolic BP	Diastolic BP	Proteinuria	Gestational Age at Delivery	Birth weight	Delivery method	fetal sex	Growth %ile	Notes
CTL-10	Hispanic or Latino	21	33.7	150	90	21	31.4	1850	NSVD	male	48%	
CTL-11	Black or African American	40	39.5	177	104	62	33	1850	NSVD	male	13%	
CTL-13	Hispanic or Latino	30	29	156	82	54	30.2	1400	C/S	male	15%	
CTL-14	Not Hispanic or Latino	37	40.4	165	85	12	31.4	1265	C/S	female	<1%	growth restricted
CTL-15	Hispanic or Latino	35	33.4	163	107	36	28.1	930	NSVD	female	3%	growth restricted
CTL-16	Not Hispanic or Latino	37	33.76	205	99	320	33.3	1970	C/S	male	17%	

Table S2C. Antibodies employed in this study, related to Figures 3, 5 and S4

Antibody	Cat #	Source	Dilution	Figure
CK7	7D3	Damsky et al., 1992	1:200	3, 5, S4
H3K4me1	07-431	Millipore	1:500-1000	S4
H3K4me3	C4208	Cell Signaling	1:500-1000	3, 5, S4
H3K9ac	Ab10812	Abcam	1:500-1000	S4
H3K9me3	Ab8898	Abcam	1:500-1000	3, 5, S4
H3K27me3	CS200603	Millipore	1:500-1000	3, 5, S4
H3K27ac	Ab4729	Abcam	1:500-1000	3, 5, S4
Pan-H3	Ab1791	Abcam	1:500-1000	3, 5, S4
TRITC	712-025-153	Jackson Immuno Research	1:100	3, 5, S4
FITC	711-095-152	Jackson Immuno Research	1:100	3, 5, S4
HRP	711-035-152	Jackson Immuno Research	1:5000	3, 5, S4